Fungal Genetics and Biology 161 (2022) 103699

Contents lists available at ScienceDirect

Fungal Genetics and Biology

journal homepage: www.elsevier.com/locate/yfgbi

Visualising long distance sugar transport in fungi using infrared fluorescence scanning imaging

Robert-Jan Bleichrodt *, Han A.B. Wösten

Microbiology, Department of Biology, Utrecht University, Utrecht, The Netherlands

ARTICLE INFO

Keywords:
Fungi
Long distance transport
Deoxyglucose
IRDye
Fluorescence imaging

ABSTRACT

Mycelia of saprotrophic basidiomycetes can cover large areas in nature that are typified by their heterogeneous nutrient availability. This heterogeneity is overcome by long distance transport of nutrients within the hyphal network to sites where they are needed. It is therefore key to be able to study nutrient transport and its underlying mechanisms. An IRDye-conjugate was used for the first time for imaging transport in fungi. A method was set up for time-lapse, high spatial resolution infrared imaging of IRDye-labelled deoxyglucose (IRDye-DG) in *Schizophyllum commune* and *Agaricus bisporus*. Scanning imaging visualised the tracer in individual hyphae as well as deeper tissues in mushrooms (mm-cm depth). The advantage of using fluorescence scanning imaging of IRDye in contrast to radiolabelled tracers studies, is that a higher spatial resolution and higher sensitivity (244 fg/ml) can be obtained. Moreover, it has a large field of view (25 × 25 cm) compared to microscopy (μm-mm range), allowing relatively fast and detailed imaging of large dimension samples.

1. Introduction

The hyphal networks of saprotrophic basidiomycetes can cover vast areas in nature. These areas are notoriously patchy in nutrient availability. Therefore, efficient nutrient distribution within the mycelium is key to continue foraging for novel food supplies and to redistribute remaining resources when essential nutrients are depleted (Heaton et al., 2020). Tip-directed mass flow facilitates nutrient transport to the parts of the network that grow, such as hyphae at the colony margin (Heaton et al., 2010), developing mushrooms (Herman et al., 2020) or, in the case of mycorrhizal fungi, to interaction zones with the plant root (van 't Padje et al., 2021a; van't Padje et al., 2021b).

Previously, long distance (>cm) nutrient transport has been assessed by liquid scintillation counting or photon counting scintillation imaging (PCSI) using radiolabelled nutrients (e.g. ^{14}C-glucose) or nutrient analogues (e.g. ^{14}C-3-O-methyl glucose or ^{14}C-aminoisobutyric acid [AIB]) (Amir et al., 1994; Tlalka et al., 2002; Herman et al., 2020). Alternatively, transport has been monitored with mass spectrometry using heavy isotopes such as ^{13}C-glucose (Jacobs et al., 2004) or with fluorescence microscopy or plate readers using fluorescently labelled nutrients such as quantum-dot tagged apatite and phosphorus (van't Padje et al., 2021a, b). However, each of these techniques has its limitations since they are destructive and therefore cannot be used for imaging *in vivo*, lack spatiotemporal resolution, have a limited field-of-view and / or have a low penetration depth. This limits the study of nutrient transport in fungal networks. Recently, fluorescence scanners have become available, similar to A4 sized flatbed document scanners, that are used to image nucleic acid or protein gels, or tumours in mice. In this study, this type of scanner is used to time-lapse monitor long distance transport of an infrared fluorescently labelled glucose analogue in the vegetative mycelium of *S. commune* and mushrooms of *A. bisporus* at μm resolution. This new method allows for deep tissue imaging, due to the high penetration depth of infrared light in tissues. In addition, the fluorescently labelled nutrients can be localised in a large field of view (FOV up to 25 × 25 cm) or in 3-dimensional samples in a shorter amount of time per surface area when compared to fluorescence microscopy and at a higher spatial resolution (21 μm) than photon counting scintillation imaging (mm). Moreover, the scintillation screens that are used for PCSI have been discontinued by the manufacturer, which makes this technique obsolete. Fluorescence scanning imaging is thus particularly suited to image nutrient transport in large microcosms such as semi-3-dimensional (3D) mushroom forming cultures or mycorrhizal interaction cultures, where not a particularly high temporal resolution is required, but rather a large FOV at a relatively high spatial resolution. Table 1 summarizes the (dis)advantages of this technique over the state-of-the-art.

* Corresponding author at: Padualaan 8, 3584 CH, Utrecht, The Netherlands.
E-mail address: r.bleichrodt@uu.nl (R.-J. Bleichrodt).

https://doi.org/10.1016/j.fgb.2022.103699
Received 15 July 2021; Received in revised form 21 April 2022; Accepted 22 April 2022
Available online 27 April 2022

Table 1
Advantages and disadvantages of PCSI, fluorescence microscopy and fluorescence scanning imaging to visualise long distance transport. Fluorescence scanning imaging is particularly useful for large samples, which may be 3-dimensional, where a high spatial resolution is required, but a high temporal resolution is not essential. Fluorescence microscopy is useful for imaging fast transport at small scale, while PCSI is useful in 2-dimensional samples where a high spatial resolution is not essential. *If spatial resolution is less of an issue a full 25 × 25 cm auto gain scan can be performed within 30 min (at 337 μm/pixel).

	PCSI	Fluorescence microscopy	Fluorescence scanning imaging
Spatial resolution (single cell analysis)	No (230 μm/pixel; Tlalka et al., 2002)	yes	almost (21 μm current study), but newer scanner models allow this (5 μm)
FOV	> 25 cm	Few hundred μm to a few mm when using stitching	25 cm
Sensitivity	^{14}C-AIB, 45 pmol label, 30 min/image, pixel size 230 μm, 12 cm Petri dish (Tlalka et al., 2002) Pixel dwelling time 6.9 ms/pixel	2-NBDG, 200 nmol label, 4.2 s/image, pixel size 0.36 μm, 35 mm glass bottom dish (Bleichrodt et al., 2015) Pixel dwelling time 1.6 μs/pixel	IRDye-DG, 734 fmol – 3.67 pmol label, 7 min/image, pixel size 337 μm, 12 cm Petri dish (this study) Pixel dwelling time 3.3 ms/pixel
Deep tissue imaging	^{14}C no, unless ^{32}P is used	no, unless infrared dyes are used, but still limited to working distance of objective (mm depth maximum)	Yes (mm-cm)
Time resolution	minutes	< seconds	minutes to hour*

2. Material and methods

2.1. Culturing

The monokaryotic *S. commune* strain 4.8b (Ohm et al., 2010) was grown for 2–4 d at 30 °C on minimal medium (SCMM: 20 g/l D-glucose monohydrate, 1.5 g/l L-asparagine monohydrate, 0.5 g/l $MgSO_4{\cdot}7H_2O$, 1 ml/l thiamine (0.12 g/l), 1 ml/l $FeCl_3$ (5 g/l), 2.5 ml/l phosphate buffer (184 g/l KH_2PO_4, 400 g/l K_2HPO_4) and 1 ml/l trace elements (0.06 g/l HBO_3, 0.04 g/l $(NH_4)_6MO_7O_{24}{\cdot}4H_2O$, 0.2 g/l $CuSO_4{\cdot}5H_2O$, 2.0 g/l $ZnSO_4{\cdot}7H_2O$, 0.1 g/l $MnSO_4{\cdot}4H_2O$, 0.4 g/l $CoCl_2{\cdot}6H_2O$, 1.2 g/l $Ca(NO_3)_2{\cdot}4H_2O$) with 1.5% agar for routine growth or 1.25% agarose for imaging. Agarose was used instead of agar because the latter shows autofluorescence in the infrared part of the electromagnetic spectrum. *A. bisporus* mushrooms were grown in open boxes filled with 2.5 kg colonised compost (PIII) and topped with 1 kg casing soil (CNC Grondstoffen) as previously described (Herman et al., 2020).

2.2. Imaging IRdye-DG translocation in S. commune mycelium

Glass bottom microscopy dishes (MatTek Corporation, Ashland, MA, P35G-1.5–20-C) were used for imaging IRDye-conjugated-deoxyglucose (IRDye 800CW 2-DG LI-COR; Kovar et al., 2009) transport in cultures grown at 30 °C (Fig. 1). Cultures without IRDye-DG labelling were used as negative control to assess autofluorescence. The cultures were either time-lapse imaged after 2–4 d of growth (Fig. 1A) or were directly imaged every 6 min after labelling (Fig. 1B). Cultures were imaged using an Odyssey CLx scanner (LI-COR; resolution 21 μm, medium background subtraction method, focus 0.5 mm, auto gain intensity, 800 nm excitation, low or medium image quality). The relation between spatial and time resolution is shown in Table 2. To add time-lapse imaging capability to the Odyssey CLx imaging software, a MacroExpress v 3.11a software (Insight Software Solutions) script (File S1) was used to allow imaging 5 positions of 2 cm^2 sequentially every 6 min. Data was exported as zip archive, while tif files of a single time-lapse sequence were loaded in Fiji (ImageJ) with the Bio-Formats plugin using a bespoke Fiji macro (File S2). Time-lapse images were converted to a stack and image analysis was performed using standard Fiji tools.

To study long distance transport, *S. commune* was grown in 12 × 12 cm Petri dishes. To this end, a 12 mm round glass coverslip was placed in the middle or on one side of 50 ml solidified SCMM agarose (see Fig. 2), on top of which a block of agar culture was placed as inoculum. In this way, label added on top of the inoculum was not in direct contact with the medium, thereby preventing its diffusion into the medium. After 8 d of growth at 30 °C the mycelium on the agarose medium, but not the inoculum, was submersed in physiological salt solution (0.9 % NaCl) with or without 0.02% sodium azide to stop growth (fungistatic; Herrick and Kempf, 1944). The latter was to test for extracellular wicking of the dye along the hyphae. After 3 h, the physiological salt solution was removed from the cultures and the inoculum was either or not labelled with 40 μl SCMM containing 10 ng/ml IRDye-DG that had been absorbed to a Whatman disc placed on top of the inoculum. After 6 d, cultures were imaged using the Odyssey CLx scanner (resolution 337 μm, medium background subtraction method, focus 4 mm, auto gain intensity, 800 nm excitation, low image quality).

Table 2
Time resolution of the Odyssey CLx scanner depending on spatial resolution and gain for a 10 × 10 cm FOV. For time-lapse imaging, first an auto gain snapshot image was generated at 337 μm resolution to determine the intensity range of the signal. Then a time-lapse sequence with fixed gain was started to enhance time resolution compared to full auto gain time-lapse imaging. These values were obtained with settings low quality, focus 0.5 mm, and 800 nm excitation. A preview at low spatial resolution with auto gain took 90 s.

Resolution (μm)	Fixed gain (min)	Auto gain (min)
21	40	90
42	18	45
84	9	25
169	4.5	12
337	2.5	6

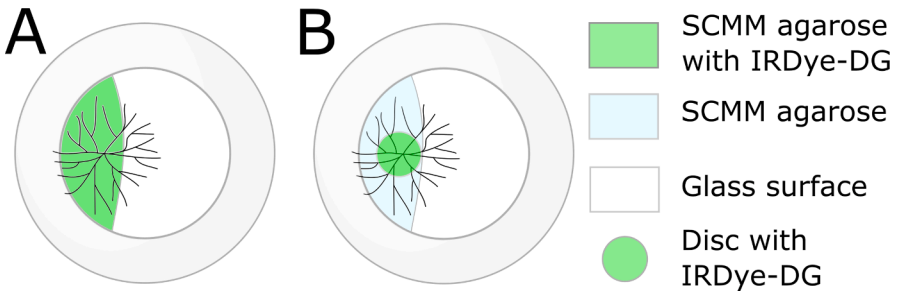

Fig. 1. Culturing *S. commune* 4.8b in 35 mm glass bottom dishes and labelling with IRDye-DG. (A) A drop of 200 μl SCMM agarose with 0.1–10 ng/ml IRDye-DG was placed at one side of the glass bottom and inoculated. The fungus was allowed to colonise the glass bottom for 2–4 d. (B) A drop of 200 μl SCMM agarose was put at one side of the glass bottom dish. After solidifying, strain 4.8b was inoculated and allowed to colonise the glass bottom. After 48 h of growth, a paper disc (Sterile disc, 10 mm, Sigma-Aldrich) was placed on top of the centre of the colony growing on the SCMM agarose, and 30–60 μl of 2 ng/ml IRDye-DG was added on top of the disc. Translocation of IRDye-DG was followed for 3 h.

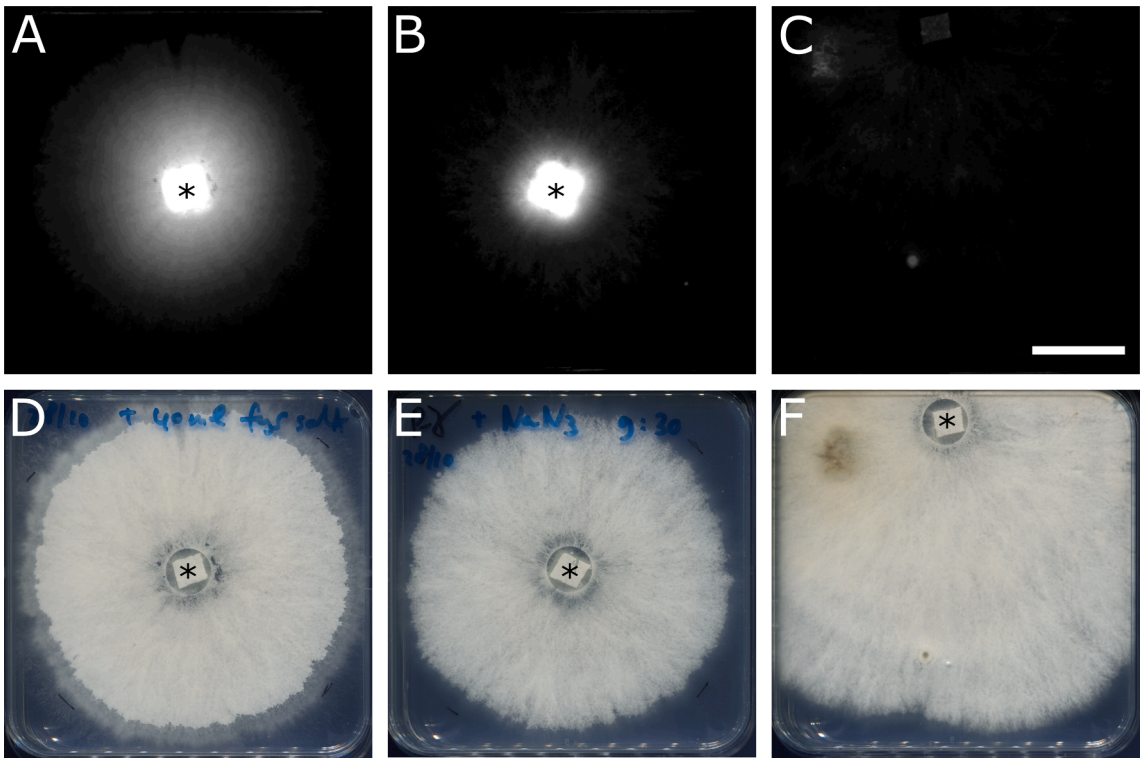

Fig. 2. Long distance intracellular IRDye-DG transport. The center of 8-day-old colonies was labelled with 40 µl 100 ng/ml IRDye-DG and incubated for 6 d (A, B). A 14-d-old non-labeled colony served as a control for autofluorescence (C). (A) Positive control showing translocation of IRDye-DG, (B) negative control incubated with sodium azide to stop growth and transport, showing no significant translocation. (D-F) bright field images of (A-C). Scale bar represents 3 cm. The inoculum is indicated with an asterisk. Images were scanned simultaneously to get the same imaging conditions.

2.3. Imaging IRDye-DG translocation in A. bisporus mushrooms

Stipes of mushrooms of *A. bisporus* were placed in 1 ml 10 ng/ml IRDye-DG aqueous solution for 1 h at RT. The bottom of the stipe was padded on tissue to remove excess of fluid, after which mushrooms were either or not longitudinally cut and placed on the mice tray of the Pearl Trilogy small animal imaging system (LI-COR) and imaged at 85 µm resolution from different angles. The advantage of the Pearl Trilogy is that it has a bright field channel, whereas the Odyssey CLx has not. Moreover, it can focus over a wide range (cm), while the Odyssey CLx can only focus maximally 4 mm deep.

2.4. Liquid scintillation counting

The inoculum of square Petri dish cultures (as Fig. 2F) was labelled with 0.5 µCi ^{14}C-AIB (2.11 GBq/mmol aqueous solution in 2% ethanol, Amersham) that had been absorbed to a piece of paper. After 8 d, ~0.5 × 1 cm pieces of agar were cut from the centre, half way between the inoculum and the colony margin, and the periphery. Agar pieces with mycelium were transferred to a LSC tube (Pony Vial 6 ml, PerkinElmer), after which 5 ml Ultima Gold™ LSC Cocktail (Merck) was added. Samples were counted two times 5 min (disintegrations per min; dpm) using a Tri-Carb 2300 TR liquid scintillation analyser (Packard).

2.5. Calculating translocation velocity and statistical analysis

The translocation velocity of IR-Dye was calculated by taking the distance from the labelling zone to the colony margin, which was divided by the time that it took for the IR-Dye fluorescence intensity to become above the background signal. The 95% confidence interval (CI) was calculated as follows $CI = z\frac{s}{\sqrt{n}}$, where z = 95% confidence level value = 1.96, s = sample standard deviation, n = number of observations.

3. Results

3.1. Imaging sugar transport in S. commune vegetative mycelium

Fluorescence intensity of IRDye-conjugated-deoxyglucose (IRDye-DG) solutions (2-fold dilutions in 100 µl water in a 96 wells plate starting with 1 ng/ml) was assessed to determine sensitivity of detection using an Odyssey CLx scanner. This showed that 244 fg/ml was still detectable (data not shown). Next, strain 4.8b was grown in glass bottom dishes with SCMM agarose with 1 ng/ml IRDye-DG on one side (Fig. 1A) to assess intracellular uptake and transport of IRDye-DG and to find the optimal focussing distance of the scanner. Agarose was used since agar showed autofluorescence in the IR spectrum (data not shown). After 4 d incubation, the mycelium in the centre and at the periphery of the colony was clearly fluorescent and individual hyphae could be observed (Fig. 3A). The best focus was obtained for hyphae on the glass surface, since hyphae growing on agarose were out of reach of the maximum focussing distance of the scanner (4 mm). Next, we set out to determine the minimum detectable concentration of IRDye-DG within hyphae. Different concentrations of IRDye-DG were mixed with SCMM agarose ranging from 0.1 to 10 ng/ml (Fig. 1A). Staining and translocation was detected with all concentrations tested (Fig. 4), but 0.5–2 ng/ml was the optimal concentration, since there was minimal oversaturation, good labelling of the hyphae, and at the lowest laser intensity.

A time-lapse imaging experiment was performed to visualise translocation by adding 2 ng/ml IRDye-DG at the centre of 48-h-old colonies using a sterile paper disc. These colonies were grown to a diameter of 13 mm by inoculating a 200 µl drop of SCMM agarose and allowing the mycelium to grow on the glass bottom of the dish (Fig. 1B). Translocation of IRDye-DG was monitored over time by scanning the colonies during 3 h (Fig. 5; Supplementary movie 1). IRDye-DG reached the periphery of the colony with a translocation velocity of 1.6 µm/s (±0.15 µm/s, 95% confidence interval).

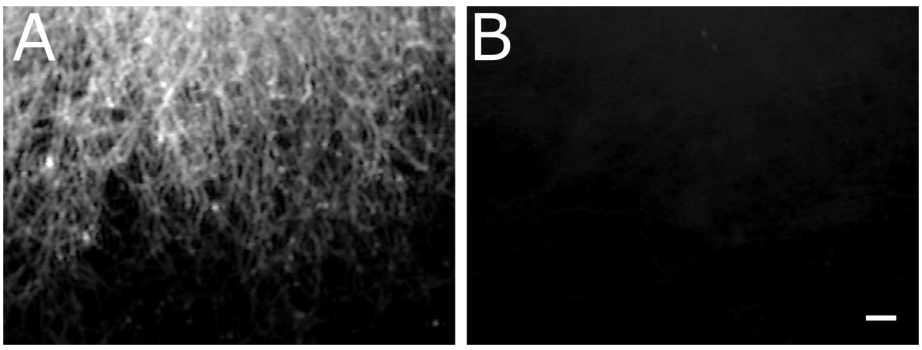

Fig. 3. IRDye-DG fluorescence in individual hyphae at the periphery of a *S. commune* 4.8b colony. (A) The fungus was inoculated and allowed to colonise the agarose drop containing 1 ng/ml IRDye-DG as well as the glass bottom of the dish during 4 d at 30 °C (see Fig. 1A). Individual labelled hyphae can be seen growing on the glass bottom. (B) A non-labelled colony served as a control. Bar represents 400 μm.

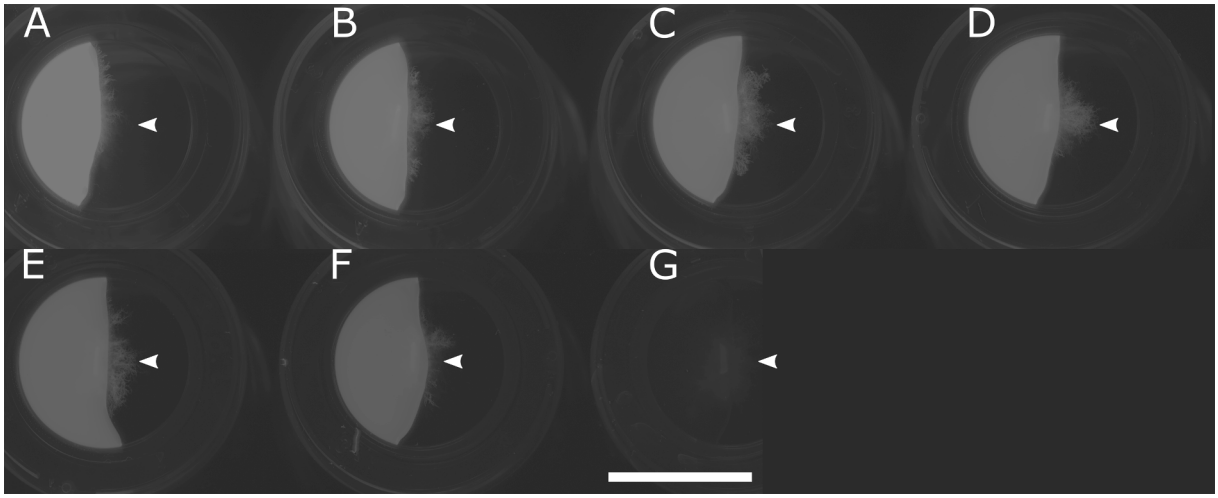

Fig. 4. IRDye-DG concentration detectable within the mycelium of *S. commune*. Strain 4.8b was grown for 48 h at 30 °C on a drop of SCMM agarose with 10 (A), 2 (B), 1 (C), 0.5 (D), 0.2 (E), 0.1 (F) or 0 (G) ng/ml IRDye-DG (see Fig. 1A). Arrow heads indicate colony margin. Scale bar represents 17.4 mm.

To test sugar translocation over longer distances, *S. commune* strain 4.8b was grown on 12 cm square Petri dishes by inoculating the centre of the medium (Fig. 2A, B). After 8 d of growth, the inoculum of the cultures was labelled with IRDye-DG after they had been treated with sodium azide to stop growth, and thereby mass flow, or with physiological salt solution as a control. In cultures treated with sodium azide, no clear translocation was observed, while control cultures did show IRDye-DG translocation. When the inoculum of 9-day-old cultures (similar to Fig. 2C) was labelled after 6 cm of radial growth and allowed to grow another 6 cm, the label translocated in 8 days to the original colony margin at the time of labelling. The translocation velocity was $\geq$ 7.5 mm per day. When the inoculum was labelled with ^{14}C-AIB, the label also did not reach the colony margin (data not shown).

3.2. Imaging sugar transport within mushrooms of A. bisporus

To test if IRDye-DG can be used to image transport in 3-dimensional fungal tissues, the stipe of *A. bisporus* mushrooms was placed in 1 ml 10 ng/ml IRDye-DG aqueous solution for 1 h at RT. The mushrooms were either or not longitudinally cut and imaged using a Pearl Trilogy small animal imaging system (LI-COR). The stipe of non-cut mushrooms showed lower fluorescence intensities than that of cut mushrooms. IRDye-DG was transported predominantly in the cortex tissue of the stipe in the direction of the cap (Fig. 6).

4. Discussion

The green fluorescent deoxyglucose analogue 2-NBDG localises to the cytosol in *Aspergillus niger* and *Coprinopsis cinerea* enabling analysis of transport of this sugar (Bleichrodt et al., 2015; Schmieder et al., 2019). Basidiomycete fungi such as *S. commune* and *A. bisporus* often show autofluorescence in the green part of the spectrum. This hampers imaging of green fluorescent molecules in general and 2-NBDG in particular in these fungi. Therefore, we here used for the first time imaging of an infrared-excitable fluorophore, IRDye-labeled deoxyglucose, in fungi to study sugar transport. The additional benefit is that exciting with infrared light is much less phototoxic than using light with lower wavelengths (Kim et al., 2015) and that infrared fluorescence can penetrate tissues deeper (Henderson and Morries, 2015). This conjugate was detected at 244 fg/ml in solution and $<$ 100 pg/ml in mycelium, which is much more sensitive than radioactive tracer studies that typically use ng-μg/ml concentrations (Tlalka et al., 2002; Herman et al., 2020; Table 1). Bigger samples like mushroom tissue could even be imaged using the Pearl Trilogy small animal imaging system (LI-COR). Henderson and Morries (2015) found that similar lasers were able to penetrate lamb brain through the skull at 1% of the initial power at a 30 mm depth. However, for fluorescence imaging, the signal has to pass back through the sample to the detector, reducing signal intensity. IRDye-DG is commonly used to detect subcutaneous tumours in nude murine models (Cheng et al., 2006), indicating that imaging within a few mm thick sample is possible. Indeed, still 20% of the original laser

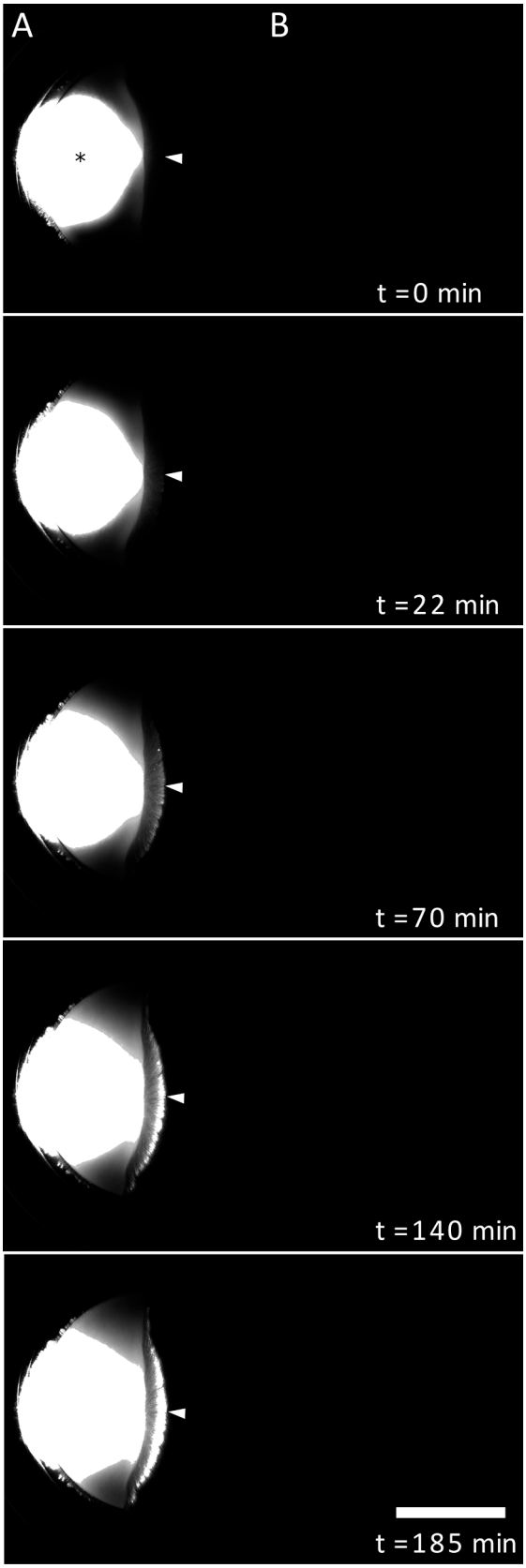

Fig. 5. Time-lapse series of IRDye-DG translocation within the mycelium of *S. commune*. A drop of SCMM agarose was placed on one side of the dish and strain 4.8b was inoculated (position indicated by *) and allowed to grow for 48 h at 30 °C. Then a 10 mm paper disc was placed on the center of the colony (indicated by asterisk) and 2 ng/ml IRDye-DG (A) or physiological salt solution, as a negative control, (B) was placed on the disc at t = 0 (see Fig. 1B). IRDye-DG translocation was observed at room temperature over time towards the colony margin (A). Arrow heads indicate colony margin. IRDye-DG accumulates in the leading hyphae over time, since translocation is faster than the growth rate. Bar represents 10 mm.

(caption on next column)

power was measured after passing through 2 mm thick sheep's skin (Henderson and Morries, 2015). These data support our notion that imaging through a few mm-cm thick fungal tissue is possible with our method. However, mushroom tissues such as the mushroom stipe can easily exceed a centimetre dimension. Indeed, signals of 2 cm wide stipes were lower when imaged as a whole when compared to samples that had been cut longitudinally, indicating that either the laser light cannot reach the medulla of the stipe or some but not all IRDye-DG fluorescence can penetrate mushroom tissue back from the medulla to the exterior of the mushroom, since the stipe diameter was ~ 2 cm.

We found similar translocation rates in the basidiomycetes *S. commune* (1.6 μm/s) and *A. bisporus* (1.8 μm/s; Herman et al., 2020), while in *A. niger* and *Neurospora crassa* higher rates have been observed (10–15 and 5–60 μm/s, respectively; Bleichrodt et al., 2013; Lew, 2005). *S. commune and A. niger* have similar growth rates. Therefore, according to the growth induced mass flow model (Heaton et al., 2010), we expected that *S. commune* would have similar translocation rates as *A. niger*. However, this was not observed. Of note, basidiomycetes have dolipore septa that can be plugged with proteinaceous material (van Driel et al., 2007; van Peer et al., 2009; van Peer et al., 2010), while ascomycetes plug their septa with Woronin bodies (Bleichrodt et al., 2012). This may impact translocation rates differently. Supporting this, translocation of ^{14}C-labeled glucose and maltose was similar in the wild type and the *hexA* mutant of *A. niger*, the latter exhibiting severely reduced septal plugging rates (Bleichrodt et al., 2015).

The fact that we did not observe any significant translocation of IRDye-DG in sodium azide treated cultures indicates that transport was not via wicking of the dye externally along the hyphae. Diffusion is also excluded since the inoculum was physically separated from the medium by placing a glass coverslip in between. Surprisingly, IRDye-DG did not reach the periphery of colonies within the timeframe of the experiments, nor was any ^{14}C-AIB detected at the periphery of colonies. The fact that the non-metabolised ^{14}C-AIB molecule translocated with a similar pattern, suggests that IRDye-DG translocation is not hampered by metabolism of the molecule or by the relatively large fluorophore coupled to deoxyglucose. Likely, it is caused by reduced water uptake by the inoculum. The inoculum needs to take up water to enable mass flow towards the colony margin (see Herman and Bleichrodt, 2021). Physically separating the inoculum from the medium by the glass coverslip, restricts mycelial water uptake to the block of medium which supports the inoculum. This would explain the initial transport to half way the colony when water is still available for uptake to drive mass flow, but then transport ceases when the water availability in the inoculum becomes limiting.

Our results show that IRDye-DG can be used to monitor sugar transport in fungi using 800 nm light. This dye may find many more applications. The infrared dye can be purchased with a reactive moiety in order to covalently link it to amine groups (IRDye® 800CW NHS Ester, LI-COR) or sulfhydryl groups (IRDye® 800CW Maleimide, LI-COR). This can be employed to fluorescently label and image uptake and transport of e.g. amino acids, amino sugars, and thiols. Using HPLC purification, the bound fluorescent molecule can be purified from the free label fraction (Kovar et al., 2009), and used for uptake and localisation studies. Moreover, similar dyes excitable with 700 nm light exist, which makes dual labelling and tracking of transport possible. This was

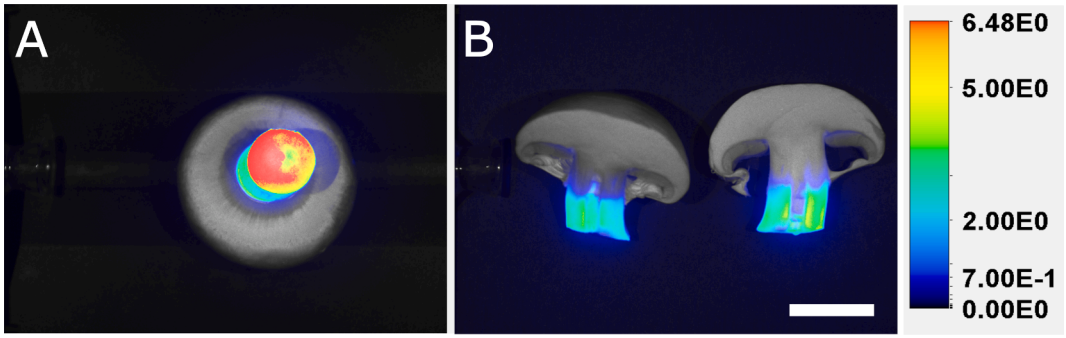

Fig. 6. IRDye-DG transport in an *A. bisporus* mushroom of strain A15. A freshly cut mushroom was hung in 1 ml 10 ng/ml IRDye-DG aqueous solution and incubated for 1 h at RT. (A) bottom view of stipe. (B) longitudinal sections showing IRDye-DG translocation predominantly in the stipe cortex tissue. Rainbow colours indicate IRDye-DG concentration and pictures show merged images with the bright field channel. Bar represents 2.5 cm.

previously not possible using radiotracers.

Overall, our method can help to unravel *in vivo* transport of nutrients and metabolites, including their directionality, quantity, and speed. This can not only be done in a 2-dimensional mycelium but also in 3D samples such as mushrooms. In addition, it can be used to trace whether specific hyphae, hyphal structures or tissues are involved in the transport process.

5. Conclusions

With this novel imaging technique:

1. Transport of nutrients can be monitored from the fungal network to mushrooms or from or to plants roots in case of mycorrhizal interactions. To our knowledge this has never been done in a large scale setup at such a relatively high spatial resolution.
2. Besides IRDye-DG, also amino acids can be fluorescently labelled to study their transport. This enables us to assess whether sugar and amino acid transport have different routes or destinations. Labels of 700 nm and 800 nm emissions are available, thus sugars and amino acids can be monitored simultaneously by exciting with two distinct wavelengths.
3. Large colonies can be monitored, while still being able to study the contribution of single hyphae in nutrient uptake. This allows us to study if all hyphae or only specific hyphae within distinct zones in the colony contribute in uptake and transport of nutrients.

This method is better suited than existing ones to address these questions because of its:

1. Better penetration depth of the signal enabling for instance to study nutrient transport within mushrooms *in vivo*.
2. Large FOV with high spatial resolution imaging.
3. Higher spatial resolution than PCSI. Moreover, the scintillation screens needed for PCSI have been discontinued.

The limitations of this new method are:

1. The time resolution is low when imaging at high spatial resolution. Therefore, this technique cannot be used to study short distance transport in single hyphae. This transport is too fast to capture at this level of detail. In this case fluorescence microscopy is best.
2. There is no optical sectioning in the Z-axis as used in confocal microscopy. Only limited spatial resolution in Z can be acquired by adjusting the focusing depth.

The open questions that cannot be answered with previous methodology and to which degree this new method expands our abilities to overcome these limitations are:

1. Visualising which cords facilitate transport to mushrooms. PCSI only measures cords at the substrate surface, since ^{14}C has a very limited penetration depth, while infrared light can pass through deeper layers of the culture. It can measure fluorescence inside living mushrooms without having to cut them in slices.
2. The velocity and amount of nutrient transport within mycorrhizal networks can be imaged over long distances. Previously, destructive techniques have been employed.
3. Simultaneous foraging behaviour for nitrogen and carbon can be visualised, using 700 and 800 nm excitable dyes. Using radiotracers, only one type of molecule can be discriminated at a time using PCSI or destructive methods.

CRediT authorship contribution statement

Robert-Jan Bleichrodt: Conceptualization, Methodology, Investigation, Formal analysis, Software, Writing. **Han A.B. Wösten:** Funding acquisition, Writing.

Declaration of Competing Interest

The authors declare that they have no known competing financial interests or personal relationships that could have appeared to influence the work reported in this paper.

Acknowledgements

This research was in part funded by the Dutch Research Council (NWO) TTW grant 'Traffic control' [15493]. The funder had no involvement in this work. We thank Sabrina Santos Oliveira and Koen Herman for assisting with imaging mushrooms using the Pearl Trilogy imager.

Declaration of interest

The authors declare to have no competing interests.

Appendix A. Supplementary data

Supplementary data to this article can be found online at https://doi.org/10.1016/j.fgb.2022.103699.

References

Amir, R., Levanon, D., Hadar, Y., Chet, I., 1994. The role of source-sink relationships in translocation during sclerotial formation by *Morchella esculenta*. Mycol. Res. 98, 1409–1414. https://doi.org/10.1016/S0953-7562(09)81071-X.

Bleichrodt, R.J., van Veluw, G.J., Recter, B., Maruyama, J., Kitamoto, K., Wösten, H.A.B., 2012. Hyphal heterogeneity in *Aspergillus oryzae* is the result of dynamic closure of

septa by Woronin bodies. Mol. Microbiol. 86, 1334–1344. https://doi.org/10.1111/mmi.12077.

Bleichrodt, R., Vinck, A., Krijgsheld, P., van Leeuwen, M.R., Dijksterhuis, J., Wösten, H. A.B., 2013. Cytosolic streaming in vegetative mycelium and aerial structures of *Aspergillus niger*. Stud. Mycol. 74, 31–46. https://doi.org/10.3114/sim0007.

Bleichrodt, R.J., Vinck, A., Read, N.D., Wösten, H.A.B., 2015. Selective transport between heterogeneous hyphal compartments via the plasma membrane lining septal walls of *Aspergillus niger*. Fungal Genet. Biol. 82, 193–200. https://doi.org/10.1016/j.fgb.2015.06.010.

Cheng, Z., Levi, J., Xiong, Z., Gheysens, O., Keren, S., Chen, X., Gambhir, S.S., 2006. Near-infrared fluorescent deoxyglucose analogue for tumor optical imaging in cell culture and living mice. Bioconjug. Chem. 17, 662–669. https://doi.org/10.1021/bc050345c.

Heaton, L.L., López, E., Maini, P.K., Fricker, M.D., Jones, N.S., 2010. Growth-induced mass flows in fungal networks. Proc. Biol. Sci. 277, 3265–3274. https://doi.org/10.1098/rspb.2010.0735.

Heaton, L.L.M., Jones, N.S., Fricker, M.D., 2020. A mechanistic explanation of the transition to simple multicellularity in fungi. Nat. Commun. 11, 2594. https://doi.org/10.1038/s41467-020-16072-4.

Henderson, T.A., Morries, L.D., 2015. Near-infrared photonic energy penetration: can infrared phototherapy effectively reach the human brain? Neuropsychiatr. Dis. Treat. 11, 2191–2208. https://doi.org/10.2147/NDT.S78182.

Herman, K.C., Bleichrodt, R., 2021. Go with the flow: mechanisms driving water transport during vegetative growth and fruiting. Fungal Biol. Rev. https://doi.org/10.1016/j.fbr.2021.10.002 in press.

Herman, K.C., Wösten, H.A.B., Fricker, M.D., Bleichrodt, R., 2020. Growth induced translocation effectively directs an amino acid analogue to developing zones in *Agaricus bisporus*. Fungal Biol. 124, 1013–1023. https://doi.org/10.1016/j.funbio.2020.09.002.

Herrick, J.A., Kempf, J.E., 1944. A study of the fungistatic and fungicidal properties and of the toxicity for mice of sodium azide. J. bacteriol. 48, 331–336. https://doi.org/10.1128/jb.48.3.331-336.1944.

Jacobs, H., Boswell, G.P., Scrimgeour, C.M., Davidson, F.A., Gadd, G.M., Ritz, K., 2004. Translocation of carbon by *Rhizoctonia solani* in nutritionally-heterogeneous microcosms. Mycol. Res. 108, 453–462. https://doi.org/10.1017/s0953756204009840.

Kim, K., Park, H., Lim, K.M., 2015. Phototoxicity: its mechanism and animal alternative test methods. Toxicol. Res. 31, 97–104. https://doi.org/10.5487/TR.2015.31.2.097.

Kovar, J.L., Volcheck, W., Sevick-Muraca, E., Simpson, M.A., Olive, D.M., 2009. Characterization and performance of a near-infrared 2-deoxyglucose optical imaging agent for mouse cancer models. Anal. Biochem. 384, 254–262. https://doi.org/10.1016/j.ab.2008.09.050.

Lew, R.R., 2005. Mass flow and pressure-driven hyphal extension in *Neurospora crassa*. Microbiology 151, 2685–2692. https://doi.org/10.1099/mic.0.27947-0.

Ohm, R.A., de Jong, J.F., Berends, E., Wang, F., Wösten, H.A.B., Lugones, L.G., 2010. An efficient gene deletion procedure for the mushroom-forming basidiomycete *Schizophyllum commune*. World J. Microbiol. Biotechnol. 10, 1919–1923. https://doi.org/10.1007/s11274-010-0356-0.

Schmieder, S.S., Stanley, C.E., Rzepiela, A., van Swaay, D., Sabotič, J., Nørrelykke, S.F., DeMello, A.J., Aebi, M., Künzler, M., 2019. Bidirectional propagation of signals and nutrients in fungal networks via specialized hyphae. Curr. Biol. 29, 217–228. https://doi.org/10.1016/j.cub.2018.11.058.

Tlalka, M., Watkinson, S.C., Darrah, P.R., Fricker, M.D., 2002. Continuous imaging of amino-acid translocation in intact mycelia of *Phanerochaete velutina* reveals rapid, pulsatile fluxes. New Phytol. 153, 173–184. https://doi.org/10.1046/j.0028-646X.2001.00288.x.

van 't Padje, A., Bonfante, P., Ciampi, L.T., Kiers, E.T., 2021a. Quantifying nutrient trade in the arbuscular mycorrhizal symbiosis under extreme weather events using quantum-dot tagged phosphorus. Frontiers Ecology Evolution. 9 https://doi.org/10.3389/fevo.2021.613119.

van't Padje, A., Oyarte Galvez, L., Klein, M., Hink, M.A., Postma, M., Shimizu, T., Kiers, E.T., 2021b. Temporal tracking of quantum-dot apatite across in vitro mycorrhizal networks shows how host demand can influence fungal nutrient transfer strategies. ISME J. 15 (2), 435–449. https://doi.org/10.1038/s41396-020-00786-w.

van Peer, A.F., Müller, W.H., Boekhout, T., Lugones, L.G., Wösten, H.A.B., 2009. Cytoplasmic continuity revisited: closure of septa of the filamentous fungus *Schizophyllum commune* in response to environmental conditions. PloS One 4, e5977. https://doi.org/10.1371/journal.pone.0005977.

van Driel, K.G., van Peer, A.F., Wösten, H.A.B., Verkleij, A.J., Boekhout, T., Müller, W.H., 2007. Enrichment of perforate septal pore caps from the basidiomycetous fungus *Rhizoctonia solani* by combined use of French press, isopycnic centrifugation, and Triton X-100. J. Microbiol. Methods 71, 298–304. https://doi.org/10.1016/j.mimet.2007.09.013.

van Peer, A.F., Wang, F., van Driel, K.G., de Jong, J.F., van Donselaar, E.G., Müller, W.H., Boekhout, T., Lugones, L.G., Wösten, H.A.B., 2010. The septal pore cap is an organelle that functions in vegetative growth and mushroom formation of the wood-rot fungus *Schizophyllum commune*. Environ. Microbiol. 12, 833–844. https://doi.org/10.1111/j.1462-2920.2009.02122.x.